Applied Catalysis B: Environmental 126 (2012) 55–63

Contents lists available at SciVerse ScienceDirect

Applied Catalysis B: Environmental

journal homepage: www.elsevier.com/locate/apcatb

Active phase genesis of NiW hydrocracking catalysts based on nickel salt heteropolytungstate: Comparison with reference catalyst

Karima Ben Tayeb[a], Carole Lamonier[a,*], Christine Lancelot[a], Michel Fournier[a], Audrey Bonduelle-Skrzypczak[b], Fabrice Bertoncini[b]

[a] Université de Lille 1, Unité de Catalyse et Chimie du Solide, CNRS UMR 8181 59652 Villeneuve d'Ascq, France
[b] IFP Energies Nouvelles, Rond-point de l'échangeur de Solaize, BP3, 69390 Vernaison, France

ARTICLE INFO

Article history:
Received 13 February 2012
Received in revised form 13 June 2012
Accepted 26 June 2012
Available online 4 July 2012

Keywords:
Sulfidation
WS_2
NiW catalysts
Heteropolyanion
XPS
HRTEM
Raman
EPR

ABSTRACT

The sulfidation of supported NiW hydrotreating catalysts is followed by a combination of X-ray photoelectron spectroscopy (XPS), high resolution transmission electron microscopy (HRTEM), Raman and electron paramagnetic resonance (EPR) spectroscopy. In this work, we compared two catalysts prepared by incipient wetness impregnation from different precursors. The first one is an innovating catalyst prepared with the nickel salt of the derived lacunary Keggin heteropolyanion (HPA) $Ni_4SiW_{11}O_{39}$ and the second one is a conventional catalyst synthesized from ammonium metatungstate and nickel nitrate. The results show for both catalysts that the sulfidation of nickel and tungsten elements does not occur at the same temperature. However, a better sulfidation of tungsten and nickel atoms respectively to WS_2 and NiWS phases is observed at 400 °C for HPA precursor compared to conventional catalyst, highlighting the benefit of HPA starting material.

1. Introduction

The new severe environmental regulations and developments of fuel market lead refiners to invest in processes for heavy oil conversion. Among them, hydrocracking (HCK) is a key process that produces selectively high quality middle distillate with low sulfur content [1]. NiW/ASA catalyst is an example of catalyst which can be used in the HCK process. The active catalysts are obtained by sulfiding an oxidic precursor, which is generally prepared by incipient wetness impregnation of an ASA support with an aqueous solution containing the elements to be deposited (Ni and W), followed by drying and calcination steps. By analogy with the CoMo hydrotreatment catalysts, where the CoMoS phase is now well accepted as the active phase [2], in NiW system, the NiWS phase has been proposed to be the active phase. This phase consists in well dispersed WS_2 nanocrystallites decorated with Ni promoter atoms.

The catalyst preparation is a key step in order to improve the catalytic performance of catalysts. The proximity of both active elements (Mo or W) and promoter (Co or Ni) has been considered as a criterion for optimizing promoting effect [3,4]. Recently, new methods of preparation of the oxidic precursors have been developed in our laboratory [5–10]. They consist in preparing new starting materials based on different heteropolytungstate nickel (heteropolymolybdate cobalt) salts to improve the promoting effect of nickel (cobalt), via the proximity of Ni (Co) and W (Mo) in the heteropolyanion salts with appropriate Ni(Co)/W(Mo) ratio.

In the present work, we study the genesis of the active phase during activation process which will enable us to understand the interest of the heteropolyanion precursor used. For this study, catalysts prepared from the derived lacunary Keggin heteropolyanion (HPA) $Ni_4SiW_{11}O_{39}$ will be compared to a conventionally impregnated catalyst. A detailed characterization of the active phase genesis is given through analysis performed by transmission electron microscopy (HRTEM), X-ray photoelectron spectroscopy (XPS), Raman and electronic paramagnetic resonance (EPR) spectroscopies.

* Corresponding author at: Unité de Catalyse et Chimie du Solide, Université de Lille1, F-59652 Lille, France. Tel.: +33 320434950; fax: +33 320436561.
E-mail address: carole.lamonier@univ-lille1.fr (C. Lamonier).

0926-3373/$ – see front matter © 2012 Elsevier B.V. All rights reserved.
http://dx.doi.org/10.1016/j.apcatb.2012.06.025

2. Experimental

2.1. Preparation of the impregnating solutions

Impregnating solutions were prepared according to two different routes:

1. Conventional impregnating solution was obtained by dissolution of ammonium metatungstate (AMT) and nickel nitrate in water with a Ni/W ratio of 0.36.
2. The derived lacunary Keggin heteropolyanion solution was prepared by dissolution in water of the corresponding nickel salt. Preparation and characterization of the nickel salt $Ni_4SiW_{11}O_{39}$ in which the Ni/W ratio is fixed at 0.36 has already been described [5–7].

2.2. Preparation of the oxidic precursors

The oxidic precursors were prepared by incipient wetness impregnation of amorphous silica alumina (ASA) support [specific surface area: 367 m^2/g, total pore volume: 0.7 ml/g] with previous impregnating solutions (1) and (2). After impregnation and 2 h of maturation in a wet atmosphere in order to let the species diffuse into the ASA, the solids were dried overnight at 100 °C and then calcined at 500 °C under oxygen. The NiW/ASA catalysts used in this work contained 17 wt.% WO_3 with an atomic ratio Ni/W of 0.36. They were named NiSiW11 and RefNiW after the corresponding impregnating solutions.

2.3. Preparation of the sulfided catalysts

In order to perform the characterization of the catalysts in their sulfided form, the oxide precursors were sulfided in glass vial at atmospheric pressure under a H_2S/H_2 (15/85) mixture with a $p(H_2S)/p(H_2)$ ratio of 0.17 and a gas flow of 2 L h^{-1} g^{-1} of catalyst. The samples were heated under the sulfiding mixture at a rate of 5 °C/min up to different temperatures varying between 20 and 400 °C, and maintained at this temperature for 2 h. They were then cooled down to room temperature. The sulfided catalysts were transferred into glass vials under vacuum in order to avoid any contact with air prior to characterization. The sulfided catalysts are denoted NiSiW11-SX and RefNiW-SX, X being the sulfidation temperature in degrees Celsius.

2.4. Characterization techniques

2.4.1. XPS

The catalysts were characterized by XPS after sulfidation at different temperatures. After their sulfidation under H_2/H_2S (85/15) for 2 h between 20 and 400 °C, samples were transferred in the spectrometer chamber using a gloves bag in order to avoid any reoxidation. The powdered samples were pressed into an indium foil attached to the sample holder, which was introduced directly in the XPS spectrometer, via the connection of the glove box to the XPS transfer chamber of the spectrometer. XPS experiments were performed using a vacuum generator Escalab 220XI spectrometer equipped with a monochromatic Al Kα (E = 1486.6 eV) X-ray source. The binding energies (BE) of W4f and Ni2p were determined by computer fitting of the measured spectra and referred to the C1s photopeak at 284.6 eV [11]. The binding energies were estimated within ±0.1 eV. The W4f and Ni2p spectra were decomposed using an interactive least-squares program and the fitting peaks of the experimental curves were defined using a combination of Gaussian and Lorentzian distributions. The decompositions were performed to estimate the sulfidation degree of tungsten (expressed as WS_2% of the total W) and the promotion degree of nickel (expressed as NiWS% of the total Ni). The surface quantification is based on the peak surface areas relative to each chemical species present on the surface of the solid. The methodology implemented for the decomposition of the spectra of the sulfided solids has been described elsewhere [7]. The method used is similar to that developed on the catalysts NiMo [12] and CoMo [13]. The parameters for the oxidic component in the W4f spectrum were determined from the analysis of the reference oxidic precursors. This contribution was introduced in the spectra of the sulfided solids. Other contributions were then introduced in order to fit the overall spectrum. The W4f spectra could then be decomposed into the three well-known contributions respectively attributed to W^{VI} oxide ($W4f_{7/2}$ BE = 36 eV, $W4f_{5/2}$ BE = 38.1 eV), W^{IV} sulfide (WS_2) ($W4f_{7/2}$ BE = 32.2 eV, $W4f_{5/2}$ BE = 34.3 eV) [4,14–21] and a third component usually associated to W^{V} oxysulfide WO_xS_y ($W4f_{7/2}$ BE = 33.5 eV, $W4f_{5/2}$ BE = 35.5 eV) [22–27]. Coulier et al. [22] noticed that this component could also be assigned to a WS_3 species. In Fig. 1A and B are shown two examples of W4f photopeak decomposition corresponding to sulfidations performed at 200 and 400 °C respectively. In Fig. 1A W(6+) is the predominant contribution whereas at 400 °C WS_2 is the major contribution. The percentages of WS_2, oxysulfide WS_xO_y and W(6+) are obtained through decompositions of the W4f photopeak containing these three contributions as shown in Fig. 1A. The sulfidation degree of tungsten (expressed as WS_2% of the total W) is determined using the following equation:

$$[WS_2] = \frac{I(WS_2)}{I(WS_2) + I(WO_xS_y) + I(W^{6+})} \times 100$$

where $I(x)$ represents the peak area of the species x.

For Ni, three contributions were observed (Fig. 1C) and attributed to Ni_xS_y ($Ni2p_{3/2}$ BE = 852.6 eV, $Ni2p_{1/2}$ BE = 869.8 eV), NiWS ($Ni2p_{3/2}$ BE = 853.7 eV, $Ni2p_{1/2}$ BE = 870.9 eV) and an oxidic phase ($Ni2p_{3/2}$ BE = 856.4 eV, $Ni2p_{1/2}$ BE = 873.8 eV) [12,18,28,29]. The Ni_xS_y phase may be present in two forms: NiS or Ni_3S_2 as reported in the literature [25]. The percentage of Ni_xS_y, NiWS and Ni^{2+} are obtained through decompositions of the $Ni2p_{3/2}$ photopeak containing these three contributions as shown in Fig. 1B. As an example, the amount of NiWS phase expressed as a percentage and named "promotion degree" was determined by using the following equation:

$$[NiWS] = \frac{I(NiWS)}{I(Ni^{2+}) + I(Ni_xS_y) + I(NiWS)} \times 100$$

where $I(x)$ represents the peak area of the species x.

The absence of any signal at 169.0 eV (characteristic of sulfates) indicated that no reoxidation of the sulfided catalysts occurred during the transfer of the solid from the sulfidation reactor to the XPS instrument [30,31].

2.4.2. High resolution transmission electron microscopy (HRTEM)

HRTEM was performed on a TECNAI electron microscope operating at an accelerating voltage of 200 kV equipped with a LaB_6 filament. Freshly sulfided samples were ground under an inert atmosphere and dispersed in ethanol. The suspension was collected on carbon films supported on copper grids. For statistical analysis, more than 70 photographs were taken, which enabled us to measure about 800 slabs for each sample. Statistical analysis was performed by measuring the length and stacking of the WS_2 slabs.

2.4.3. Raman spectroscopy

Raman spectra of the sulfided samples were recorded through glass vial using a Raman microprobe equipped with a photodiode array detector. The exciting laser source was the 532 nm line of a Nd-YAG laser with a beam power of 0.23 mW at the focal point. The wavenumber accuracy was 2 cm^{-1}.

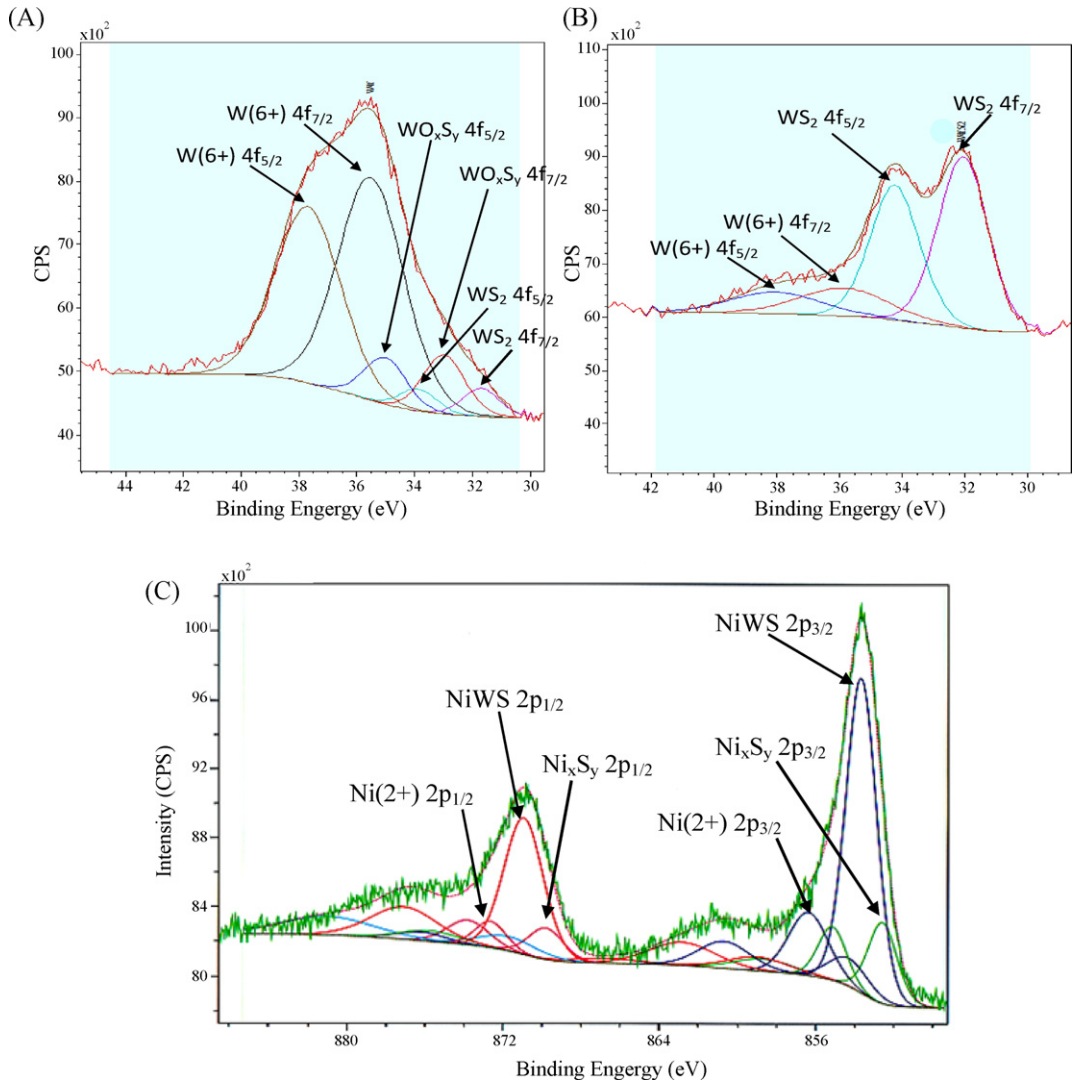

Fig. 1. Examples of decomposition of XPS spectra recorded for $NiSiW_{11}$ catalyst (A) after sulfidation at 200 °C, W4f spectrum: contribution of $W^{IV}S_2$ phase, contribution of W^{V} oxysulfide phase and contribution of W^{VI} oxidic phase. (B) After sulfidation at 400 °C, W4f spectrum: contribution of $W^{IV}S_2$ phase, contribution of W^{VI} oxidic phase (C) Ni 2p spectrum: contribution of NiWS phase, contribution of Ni_xS_y and contribution of oxidic phase.

2.4.4. EPR spectroscopy

The continuous wave (CW) X-band EPR spectra were recorded through sealed quartz tube on a Brüker ELEXYS 580-FT spectrometer. The CW spectra were recorded at 110 K and 4 K, with a modulation amplitude of 10 and 6 G respectively and a microwave power of 10 and 2.5 mW that assumes non-saturation conditions.

3. Results: genesis of the active phase

3.1. XPS characterizations

The solids sulfided at various temperatures were analyzed by XPS in order to identify and quantify the different phases (WS_2, WO_xS_y and W(6+)). Fig. 2A and B shows the evolution of the W 4f XPS spectra of NiSiW11 and RefNiW catalysts at different steps of the activation. Whatever the solid, the spectra from ambient temperature up to 200 °C are similar and exhibit two peaks (W $4f_{7/2}$: 36.3 eV, W $4f_{5/2}$: 38.5 eV) characteristic of W in an oxidic environment. During the activation of NiSiW11, the W 4f spectrum evolves continuously from 300 °C to 400 °C. Indeed, the intensity of the oxidic state W contribution (BE = 36.3 and 38.5 eV) decreases while the sulfidic state W one increases (BE = 32.5 and 34.6 eV). So the tungsten sulfidation starts at 300 °C and continues significantly up to 400 °C. For RefNiW the evolution is different: the W 4f spectrum does not evolve between 300 °C and 400 °C.

These qualitative observations are corroborated by the decompositions performed on these spectra and which results are gathered in Table 1. On both solids, the quantity of tungsten in oxidic environment noted W(6+) decreases with the increase of temperature from room temperature to 400 °C, down to 23% for NiSiW11 and 51% for RefNiW. From previous Raman spectroscopy results, this W(6+) form already observed after calcination has been found to be an amorphous tungsten oxide phase [32]. The oxysulfide quantity WO_xS_y shows a maximum between 12 and 14% at 200 °C. This phase disappears at high temperature (300 and 400 °C). For both catalysts, a low sulfidation degree of tungsten (below 10%) is observed between 20 and 200 °C. Indeed, the sulfidation degree increases when raising the activation temperature, in similar proportion for both solids (from 6% at 200 °C to 51% at 300 °C for NiSiW11 and from 10% to 49% for RefNiW). Above 300 °C, the evolution of the sulfidation degree is different on the two solids. For NiSiW11 catalyst, this value still increases at 400 °C with 77% of sulfidic WS_2 entities, while it remains at the same level that is 49%, on the RefNiW catalyst. Sun et al. [14] indicate that the

Table 1
XPS data of the NiSiW11 and RefNiW catalysts at different stages of sulfidation.

Catalysts nomenclature	WS_2 sulfidation degree (%)	WO_xS_y quantity (%)	W(6+) quantity (%)	NiWS promotion degree (%)	Ni_xS_y quantity (%)	Ni(2+) quantity (%)
NiSiW11-S20	4	8	88	0	12	88
RefNiW-S20	0	3	97	0	14	86
NiSiW11-S100	3	10	87	0	13	87
RefNiW-S100	4	5	91	0	15	85
NiSiW11-S200	6	14	80	36	30	34
RefNiW-S200	10	12	78	28	20	52
NiSiW11-S300	51	1	48	39	28	33
RefNiW-S300	49	1	50	37	30	33
NiSiW11-S400	77	0	23	42	39	19
RefNiW-S400	49	0	51	37	34	29

sulfidation degree of tungsten is 44% for a NiW/Al_2O_3 catalyst calcined at 500 °C and sulfided at 400 °C, which is coherent with the value found in our work for the reference catalyst calcined and sulfided at the same temperatures. Vissenberg et al. [33] found a sulfidation degree of 70% for NiW/Al_2O_3 catalysts, calcined and sulfided at 400 °C. They observed an improvement of the sulfidation degree (89%) when raising the activation temperature at 650 °C, but even at this high temperature the sulfidation of tungsten is not complete. Moreover, the increase of calcination temperature at 550 °C decreases the sulfidation degree (49%). Indeed, more elevated calcination temperature renders the sulfidation more difficult. The same authors also demonstrated that sulfidation of NiW/Al_2O_3 at 400 °C progresses more towards WS_2 when the sulfidation pressure is increased from 1 to 15 bar with respectively sulfidation degree of 70 and 79%. From a catalytic point of view, Vissenberg et al. [33] showed a correlation between activity and W sulfidation degree for catalysts calcined at various temperatures but when temperature or pressure sulfidation were varied, this correlation no longer held. They concluded that sulfidation degree was not the only factor determining the activity.

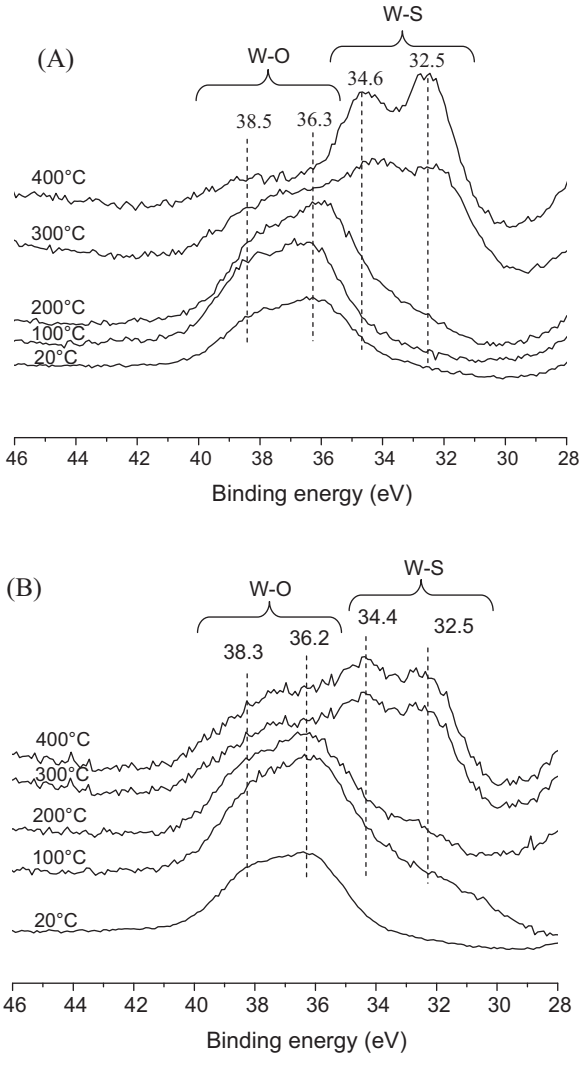

Fig. 2. XPS spectra of NiSiW11 and RefNiW at different stages of sulfidation. (A) W4f spectra for NiSiW11 catalyst and (B) W4f spectra for RefNiW catalyst.

Fig. 3A and B shows respectively the evolution of the Ni 2p XPS spectra of the NiSiW11 and RefNiW catalysts at different temperatures of sulfidation. For both solids, the Ni XPS features of the oxide components (peaks at 856.8 and 874.8 eV) gradually disappear while those of the sulfide ones appear (peaks at 853.9 and 871 eV) upon increasing the sulfidation temperature from room temperature up to 400 °C. Thus, nickel sulfidation starts at room temperature but the sulfided species mostly appear from 200 °C. In agreement with our results, Reinhoudt et al. [15] reported that nickel sulfidation into NiS phase starts at room temperature with 15% for a catalyst NiW/Al_2O_3 calcined at 400 °C.

Through careful decomposition, the amounts of Ni(2+), Ni_xS_y and NiWS phase have been determined and the corresponding quantities of the different phases are reported in Table 1. On both solids, the Ni_xS_y phase appears even at room temperature with values between 12 and 14% at 20 °C and increases with the sulfidation temperature, reaching at 400 °C respectively 34 and 39% on RefNiW and NiSiW11 catalysts. The Ni quantity in oxidic environment noted Ni(2+) decreases with the increase of temperature from room temperature to 400 °C, down to 19% for NiSiW11 and 29% for RefNiW. Reinhoudt et al. [15] indicate that the total quantity of nickel in oxide components decreases upon increasing the sulfidation temperature from room temperature up to 400 °C respectively from 82% to 15%.

The NiWS phase starts to appear at 200 °C. For RefNiW solid, a plateau is reached at 300 °C with values around 37%. For a NiW/C catalyst prepared from ammonium metatungstate and nickel nitrate, Hensen et al. [27] determined by Mössbauer emission spectroscopy that 39% of NiWS is obtained for a sulfidation temperature of 400 °C, the precursor being dried at 120 °C without calcination whereas for NiW/ASA catalyst, the same authors indicate that 48% of NiWS is obtained for a sulfidation temperature of 400 °C, the precursor being also calcined at 400 °C. It is then noted that the calcination at elevated temperature renders the sulfidation more difficult and could explain the value equal to 37% of NiWS obtained for the conventional catalyst calcined at 500 °C and sulfided at 400 °C. Nevertheless, for HPA based catalysts calcined at 500 °C, the NiWS quantity keeps on increasing for the NiSiW11 solid to achieve 42% at 400 °C. We can notice that whatever the sulfidation temperature, the quantity of NiWS phase in the case of

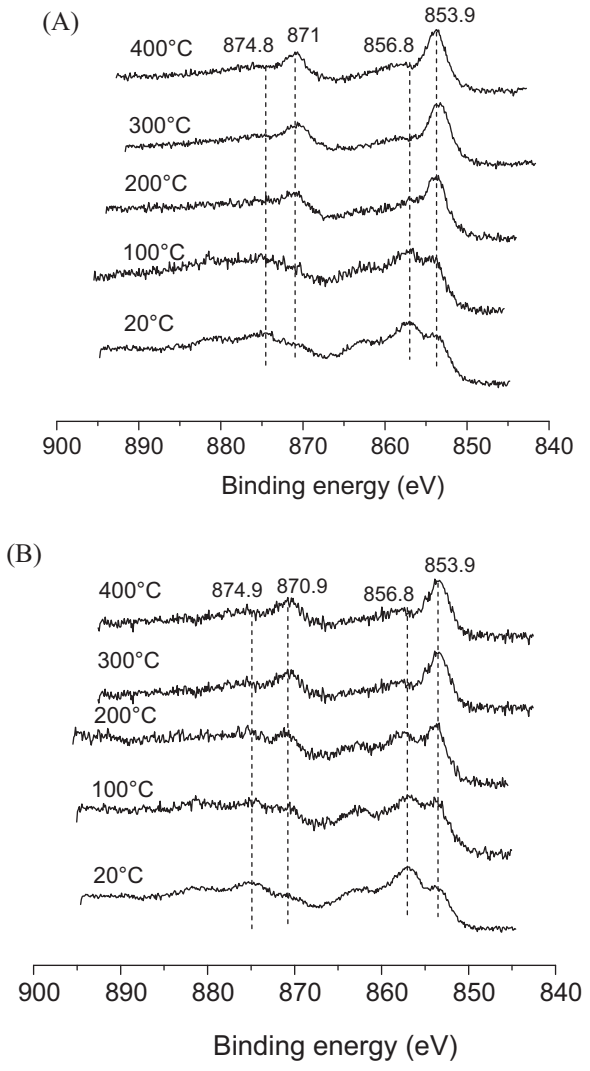

Fig. 3. XPS spectra of NiSiW11 and RefNiW at different stages of sulfidation. (A) Ni2p spectra for NiSiW11 catalyst and (B) Ni2p spectra for RefNiW catalyst.

heteropolyanion based catalysts is slightly larger than in the case of conventional precursors.

Whatever the solid, we observe that the sulfidation of tungsten and nickel atoms does not occur at the same temperature. Indeed, nickel sulfidation rapidly starts at room temperature as Ni_xS_y phase. However, tungsten sulfidation slightly begins from 200 °C. Moreover, a better sulfidation of tungsten as well as a higher quantity of NiWS phase is obtained for the catalyst based on heteropolyanion compared to the catalyst based on conventional precursor.

3.2. HRTEM

The sulfided catalysts NiSiW11 and RefNiW were analyzed using HRTEM to follow the evolution of the WS_2 morphology when increasing the activation temperature from 200 to 400 °C. Fig. 4 shows typical images recorded for the catalyst NiSiW11 sulfided at 200 °C (Fig. 4A) and at 400 °C (Fig. 4B), which are also representative of the observation performed on RefNiW sulfided catalyst. On both solids, only a few single slabs are observed at 200 °C, in agreement with the low sulfidation degree of tungsten obtained by XPS analysis. The presence of WS_2 slabs is clearly visible at 400 °C with the typical layered structure of WS_2. The observation of various photos shows a heterogeneous distribution of the slabs over the ASA support, with areas showing very few or none slabs areas with a majority of monolayers, while areas densely populated with multiple-stacked slabs were also found. This result is in agreement with previous studies in the literature, where Van Der Meer et al. [24] demonstrated by EDX analysis that the WS_2 slabs are mostly located on the alumina part of the ASA support, indicating that tungsten preferentially interacts with alumina of the support materials.

The distribution of the length and stacking degree of WS_2 slabs for NiSiW11 and RefNiW catalysts sulfided at 400 °C are reported in Fig. 5 (distributions not shown for NiSiW11 and RefNiW at 200 and 300 °C). The average slab length and stacking degree of all catalysts are listed in Table 2. Concerning the slabs stacking, single-layered slabs are predominant as reported in the literature [27,33]. For both solids, at 200 °C, only single slabs were detected, their length being lower than 20 Å. Fifty-five percent of the detected slabs have a length centered on the 10–19 Å interval for NiSiW11 catalyst versus 47% for RefNiW catalyst with both an average slab length of 10 Å. At 300 °C, slabs as long as 49 Å are observed on NiSiW11, while 29 Å on RefNiW catalyst. The average slab length is 18 Å on

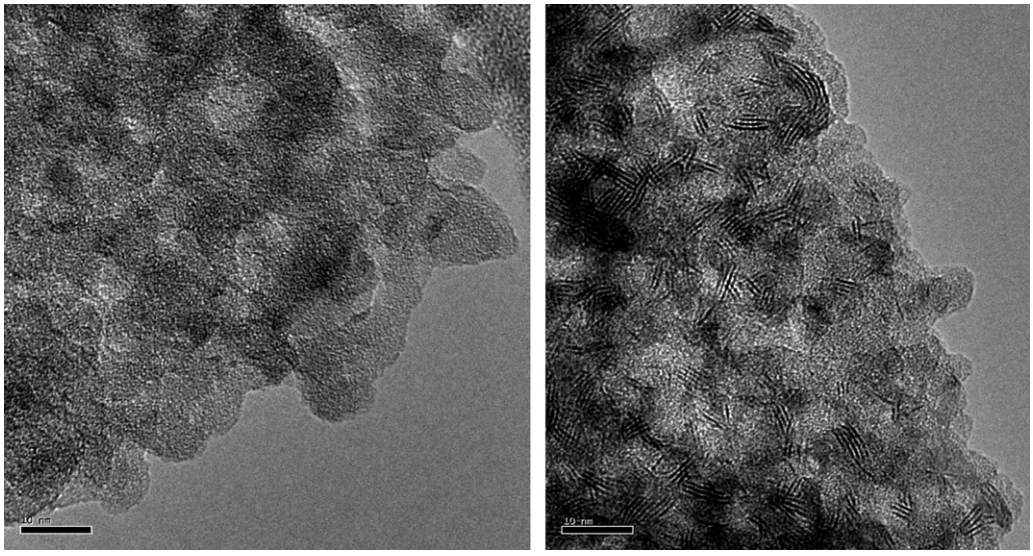

Fig. 4. Typical HRTEM micrographs of NiSiW11 catalyst sulfided at 200 °C (left) and 400 °C (right).

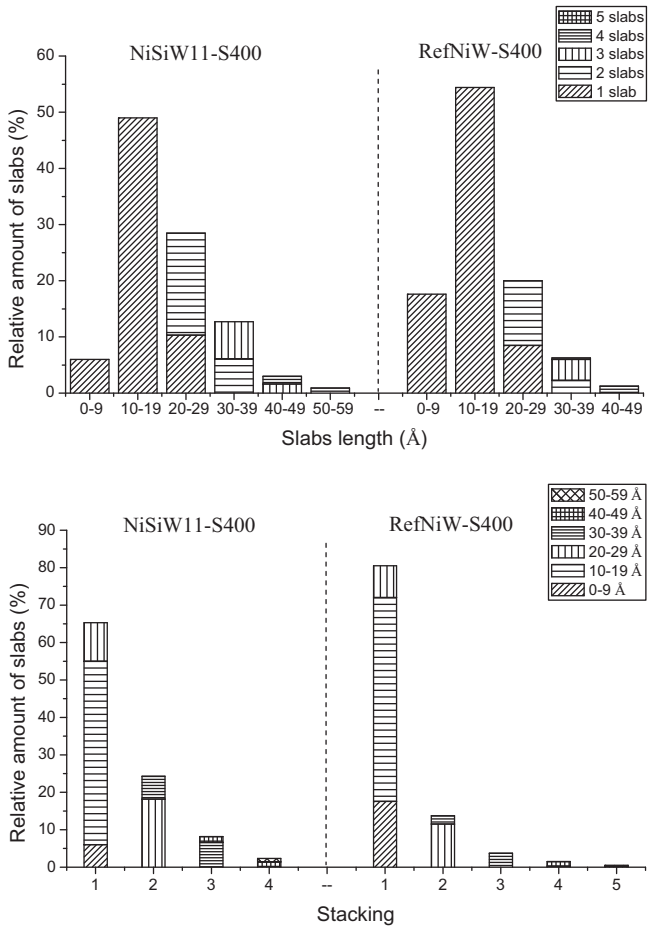

Fig. 5. Distribution of the length and stacking of the WS_2 slabs of the NiSiW11 and RefNiW catalysts after sulfidation at 400 °C for 2 h.

catalyst based on heteropolyanion against 12 Å for the conventional catalyst while the stacking of the WS_2 slabs is identical with an average slab stacking of 1.3. Concerning the sulfidation at 400 °C, the slab length distribution is centered for both catalysts on the 10–19 Å interval but the average slab length is higher for NiSiW11 catalyst with respective average values of 21 and 17 Å for NiSiW11 and RefNiW catalysts. The average slab stacking is slightly higher for NiSiW11 with 1.5 versus 1.3 for the conventional catalyst. As mentioned in a previous study [7], the WS_2 average slab length supported on ASA material containing 90% of silica and 10% of alumina, with a Ni/W ratio of 0.36 is smaller than those reported in the literature [24,27,33] where the WS_2 active phase is dispersed on different supports such as alumina, carbon or different ASA, with catalysts having a Ni/W ratio of 0.25. Assuming that the NiWS active sites are located at the edges of the WS_2 hexagonal slabs in the plane of W atoms, the smaller the WS_2 slabs, the larger the possible relative number of active sites (NiWS/total amount of WS_2). Smaller WS_2 crystallites could then be beneficial to catalytic activity from a geometric point of view. This geometric model has been proposed by Kaztelan [34]. The specific nature of the hydrogenation sites in sulfided hydroprocessing catalysts is still a matter of debate. Nevertheless, the rim-edge model proposed by Daage and Chinelli [35] suggested that hydrogenation of large molecule would occur on the rim sites located at the top and the bottom of stacked slabs where more room is available for flat adsorption. Taking into account these two points, average length and stacking are two data characterizing WS_2 phase and being related to catalytic properties.

Table 2
Average slab length, average stacking degree of studied catalysts.

Catalysts nomenclature	Average slab length (Å)	Average stacking degree
NiSiW11-S200	10	1
RefNiW-S200	10	1
NiSiW11-S300	18	1.3
RefNiW-S300	12	1.3
NiSiW11-S400	21	1.5
RefNiW-S400	17	1.3

When raising the sulfidation temperature, an increase of the slabs length and stacking is observed whatever the catalyst. However, the evolution is different for NiSiW11 and RefNiW. At 200 °C, a similar average slab length is observed for both catalysts, with a value of 10 Å and an average stacking of 1. When the sulfidation temperature is raised to 300 °C, an increase in the slab length is observed for both catalysts with a strong evolution for NiSiW11 catalyst (from 10 to 18 Å) and a moderate evolution for the RefNiW catalyst (from 10 to 12 Å). However, the average slab stacking remains identical (1.3). From 300 °C to 400 °C, the slabs length for NiSiW11 catalyst does not evolve much, from 18 to 21 Å with an increase of the stacking from 1.3 to 1.5, while a strong increase is observed for the RefNiW catalyst, from 12 to 17 Å with a constant stacking (1.3). Van Der Meer et al. [24] indicate that increasing of the sulfidation temperature (400–650 °C) leads to a strong growth of the lateral dimensions of the WS_2 slabs (29–44 Å) and a small increase in stacking degree (1.1–1.5) for NiW/ASA catalysts. The same conclusions are reported by Hensen et al. [27] for NiW/Al_2O_3 catalysts. Indeed, the higher sulfidation temperature (650 °C instead of 400 °C) did not affect the stacking degree (1.3) but resulted in an increase in slab length respectively from 33 Å to 42 Å.

3.3. Raman spectroscopy

Fig. 6A shows the Raman spectra of the NiSiW11 after sulfidation at different temperatures. The spectra are similar for the temperature from room temperature to 100 °C. The lines at 291, 334, 377, 471, 536 and 566 cm^{-1} are characteristic of the presence of oxysulfide entities [36]. The well-defined line at 471 cm^{-1} could be assigned to a stretching vibration of the W—S bond while the lines at 377 and 566 cm^{-1} could be corresponded to a W—O vibration bond in an oxysulfide phase [36]. However, no vibration band assigned to the W—O bond is observed in the region 800–1000 cm^{-1} because the intensity of this line is known to be very low in oxysulfides compounds as reported in the case of $W_3OS_8^{2-}$ anion Raman analysis [37]. In the same way, W—O terminal vibration bands of the WO_3 phase are also not visible in the 800–1000 cm^{-1} region due to a very low relative intensity compared to W—S band vibration. At 200 °C WS_3 is identified by a characteristic broadening of the whole Raman spectrum together with a variation of the intensity of the bands at 293 and 471 cm^{-1}. This assignment is in agreement with Payen et al. [36]. The lines at 374, 471 and 569 cm^{-1} are still observed, which suggests that a part of the oxysulfide phase is preserved. At 300 and 400 °C, the spectra exhibit additional lines at 350 and 413 cm^{-1} which indicate the presence of WS_2 phase [36]. A careful examination of Raman spectrum at 300 °C taking into account the intensity and broadening of the peaks could suggest the simultaneous presence of WS_2, WS_3 and WO_xS_y entities. Tungsten oxysulfide characteristic features were unambiguously noticed in Raman spectra at 20 and 100 °C with peaks at 291, 334, 377 and 471 cm^{-1}. These spectra were dominated by the peaks at 291 and 471 cm^{-1}, this latter being the most intense. When oxysulfide species are mixed with other species as WS_2 and WS_3 as it is proposed at 300 °C, one can assume that the less intense peaks at 377 and 566 cm^{-1} corresponding to W—O vibrations could be mixed in the background of the Raman spectrum and then not

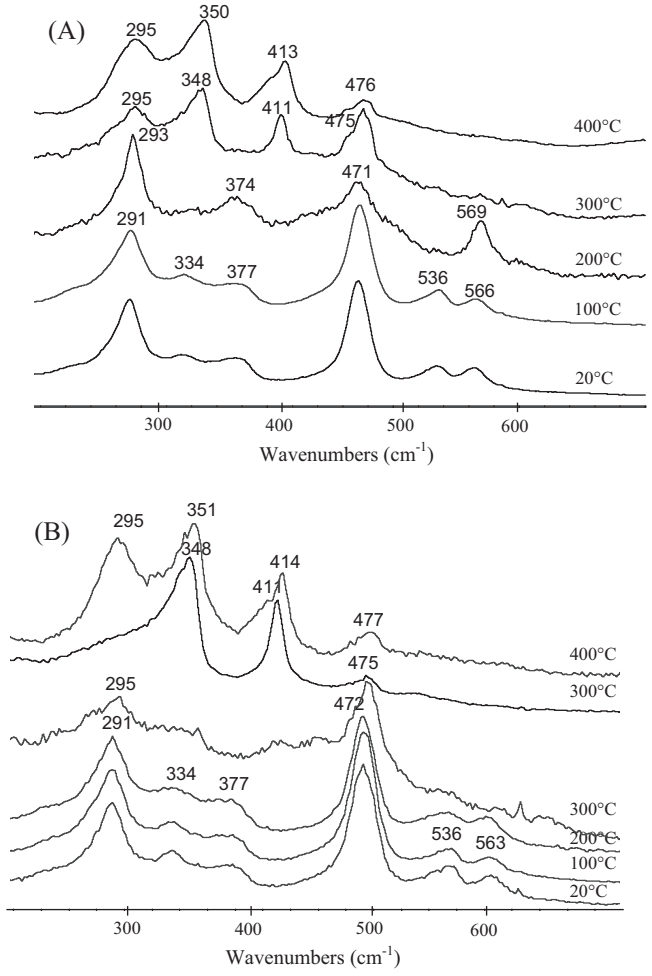

Fig. 6. Raman spectra in the 200–700 cm^{-1} spectral range of NiSiW11 (A) and RefNiW (B) catalysts at different stages of sulfidation.

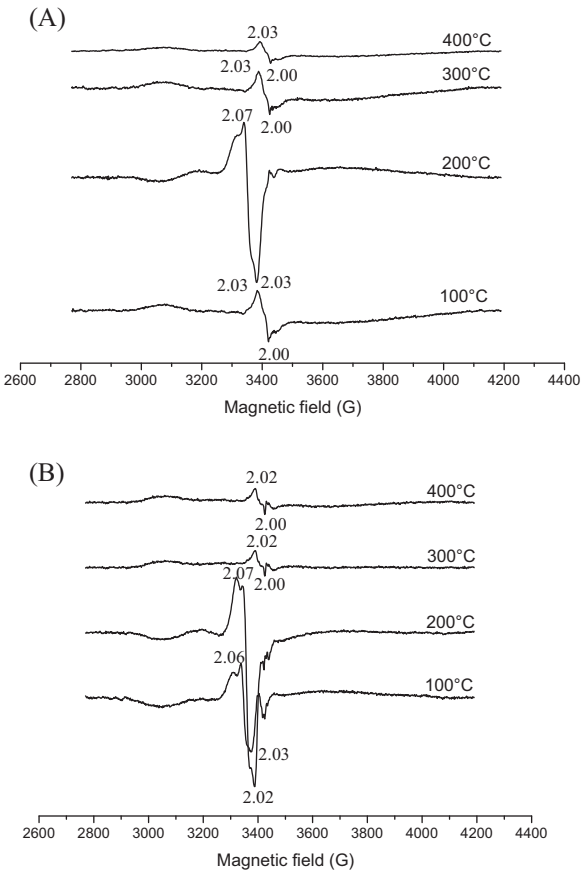

Fig. 7. EPR spectra of NiSiW11 (A) and RefNiW (B) catalysts at different stages of sulfidation.

visible. The high intensity of the peak at 476 cm^{-1} compared to the one of the peak at 295 cm^{-1} seems to indicate that tungsten oxysulfide species could still be present at 300 °C beside WS_3 and WS_2 and transformed into WS_3 at 400 °C.

The spectra of RefNiW catalyst (Fig. 6B) between 20 and 200 °C are similar to those observed during the sulfidation of the NiSiW11 catalyst between 20 and 100 °C, with characteristic lines of an oxysulfide phase [36]. At 300 °C, an inhomogeneous solid is observed, with two types of spectra: one shows poorly resolved main lines at 295 and 475 cm^{-1} corresponding to oxysulfide and WS_3 phase while the second exhibits lines at 348 and 411 cm^{-1} characteristic of the presence of a WS_2 phase [36]. Thus, the WS_3 phase appears later on conventional catalyst. At 400 °C, the solid is homogeneous and presents a similar spectrum to those observed for NiSiW11, which is characteristic of the presence of WS_2 and WS_3 entities. Van Der Meer et al. [24] indicate that the mode of sulfidation has some influence on the formation of the intermediate phases. They only found the presence of WS_3 intermediate after single-step sulfidation at 300 °C for NiW/ASA catalyst prepared from ammonium metatungstate and nickel nitrate calcined at 550 °C [24]. Reinhoudt et al. [38] suggested from temperature-programmed sulfidation (TPS) measurements that tungsten sulfidation in NiW/Al_2O_3 proceeds via WS_3. It is shown that the calcination temperature has a great influence on the relative importance of the different sulfidation reactions. Especially the WS_3 formation at sulfidation temperatures below 327 °C is strongly decreased after calcination above 400 °C. A WS_3 intermediate phase has also been found by TPS during sulfidation below 300 °C of the catalyst $NiATT/Al_2O_3$. This latter was prepared from ammonium tetrathiotungstate (ATT), nickel nitrate and dried at 120 °C (not calcined) [14].

3.4. EPR spectroscopy

In order to obtain more information on oxidation state of tungsten and nickel, both catalysts NiSiW11 and RefNiW were analyzed by EPR after sulfidation at different temperatures. As mentioned in the literature [23–27], an oxysulfide phase is observed during the tungsten sulfidation, where the tungsten atom could be found in an oxidation state of V or VI. As W(5+) is a paramagnetic species, it can be detected by EPR and then W(5+) has been extensively characterized using this technique [39–42]. For the elements with a low relaxation time as tungsten, it is necessary to record a spectrum at low temperature in order to obtain a more intense signal. The spectra of both catalysts were first recorded at 110 K and were respectively presented in Fig. 7A and B. For the catalyst based on heteropolyanion, a weak signal is observed at 100, 300 and 400 °C with a *g* Landé factor equal to 2.03 and an intense signal is showed at 200 °C with a *g* factor equal to 2.07. The Landé factor *g* is important because it permits to determine the nature of the chemical element. A *g* factor between 2.02 and 2.75 is attributed to nickel element, with values between 2.49 and 2.75 for Ni^+ species whereas Ni^{2+} was observed at lower values [39–42]. For tungsten element with the oxidation degree +5, this *g* factor is expected between 1.39 and 1.85 [43–47]. EPR results indicate the formation at 200 °C of an intermediate species related to nickel element with a *g* factor equal to 2.07, this species disappearing at higher temperature. For the conventional catalyst, the same intermediate species with a *g* factor equal to 2.07 appears at 100 °C and becomes more intense

at 200 °C. The observation of this signal associated to nickel based species could be related to the presence of oxysulfide entities predominantly observed at 200 °C for both catalysts by XPS and Raman spectroscopy. Therefore, nickel element being in interaction with the oxysulfide phase could be a paramagnetic entity visible by EPR and characterized by a *g* factor equal to 2.07. This phase could be sulfided to NiWS phase for temperatures higher than 200 °C, which could explain the disappearance of the EPR signals at 300 and 400 °C. In the literature [24], interaction between nickel sulfide and oxysulfide phase at relatively low sulfidation temperatures (around 200 °C) has been evidenced by EXAFS at the Ni Kedge. For a sulfidation below 200 °C, Reinhoudt et al. [15] also mentioned the presence of a Ni sulfide species in close interaction with an oxidic or partially sulfided W phase.

However, although we demonstrated by XPS and Raman the presence of oxysulfide species in which W is supposed to be at the oxidation degree +5, no signal has been observed with a *g* factor lower than 2 characteristic of tungsten element. In order to get a more intense signal for this element of low relaxation time, the same experiments have been then performed at 4 K. Results obtained at 110 K have been confirmed with no W(5+) signal detected even at 4 K. Two hypotheses could be proposed. First, the oxysulfide phase does not contain W(5+) but W(6+) invisible by EPR as already proposed in the literature [41].The reoxidation of W(5+) to W(6+) may also be considered and could also explain the absence of the signal. To definitely exclude this hypothesis, an *operando* sulfidation followed by EPR spectroscopy is under progress.

4. Discussion

In a previous study [7], we have shown the different catalytic behavior in toluene hydrogenation reaction of the two catalysts when sulfided at 350 °C. The catalyst NiSiW11 was found to be more efficient. Indeed, catalytic results show clearly that this catalyst is 30% more hydrogenating than its counterpart prepared with conventional precursor. Moreover, $Ni_4SiW_{11}O_{39}$ nickel salt as precursor led to high dispersion: its Raman spectrum showed after calcination a main peak at 975 cm^{-1} attributed to well dispersed polytungstate phase whereas no crystalline phase as WO_3 was identified. This observation was also corroborated by HRTEM analysis on the sulfided phase, where no bulk oxide phase was evidenced on TEM images whereas the sulfided WS_2 phase appeared in the form of slabs on ASA support. A higher promoting effect was also noticed in the resulting catalyst [7]. The beneficial use of $Ni_4SiW_{11}O_{39}$ has been attributed to the initial proximity of Ni and W in the heteropolyanion salt maintained after drying. The beneficial use of HPA has been also reported to prepare efficient CoMo hydrodesulfidation catalysts [8–10]. For a better understanding, we studied the genesis of active phase that describes the temperature effect on the tungsten and nickel sulfidation for the two solids. In the literature [22,26,27,30,31,48], many authors used chelating agents which permit to improve the sulfidation of both elements (Ni and W) and therefore the catalytic performance of the catalysts. Indeed, chelating agents considerably retarded the sulfidation of nickel (or cobalt) until the point where tungsten (or molybdenum) is more or less completely sulfided which permits a simultaneous sulfidation of both Ni and W atoms [22,26,27,48] or both Co and Mo atoms [30,31].

Firstly, XPS results are in agreement with the formation of WS_2 via partially sulfided WO_xS_y but do not permit to identify a WS_3 phase. Raman spectroscopy is the single technique that reveals the presence of WS_3 and WO_xS_y phases as intermediates of sulfidation. Payen et al. [36] reported that the sulfidation of tungsten is carried out with different steps as showed below:

$$WO_3 \rightarrow WO_xS_y \rightarrow WS_3 \rightarrow WS_2$$

In the literature, the sulfidation of tungsten from W(6+) oxide to W(4+) sulfide is still in debate. Some authors [14,21] indicate that a fraction of tungsten may be present in higher oxidation states either as oxysulfides or as WS_3-like species. Most authors [25,27,33,49–52] report that sulfidation of W(6+) proceeds via oxysulfide intermediates to W(4+)S_2. Other authors [14,15,22,24,38] suggested WS_3 as intermediate in the sulfidation of tungsten. The results obtained by XPS show that WS_2 proportion is lower than 10% for the two types of precursors between 20 and 200 °C. At 300 °C, the WS_2 phase is predominant and it continues to evolve for the NiSiW11 catalyst at 400 °C (NiSiW11: 77% versus RefNiW: 49%). This NiSiW11 catalyst possessing a large quantity of WS_2 phase, obtained by increasing the sulfiding temperature to 400 °C, was then evaluated in toluene hydrogenation but presented lower catalytic performances compared to that of the same catalyst sulfided at 350 °C, respectively 0.87 and 2.91 mol of converted toluene per mol of tungsten and per hour. Indeed the most important parameter is known to be the quantity of NiWS phase rather than the sulfidation rate. Similar conclusions were also reported by Vissenberg et al. [33] on NiW supported on alumina.

Analysis obtained by Raman spectroscopy are in agreement with XPS results with the observation of oxysulfide phase between room temperature and 200 °C and the predominant formation of WS_2 phase from 300 °C. In fact, the progressive sulfidation of W(6+) to WS_2 phase occurred via oxysulfide and WS_3 phases. This latter phase appears later for the conventional catalyst (300 versus 200 °C) which can explain that the tungsten sulfidation degree is lower than the NiSiW11 catalyst one. However, for both catalysts, the WS_3 phase is still present for sulfidation temperature of 400 °C. As reported in the literature [24], the tungsten sulfidation is incomplete at 400 °C with the presence of tungsten in an oxidic environment. Reinhoudt et al. [15] studied the active phase genesis by XPS of NiW/Al_2O_3 catalysts calcined at 550 °C and sulfided at various increasing temperatures. They showed the presence of W in an oxidic environment for sulfidation temperatures of 25 °C and 267 °C. At 340 °C, the sulfidic state W appeared in a small proportion while at 500 °C the WS_2 phase is predominant [15]. Indeed, the tungsten sulfidation is known to be more difficult in comparison to molybdenum [27]. Sulfidation of tungsten proceeds at a lower rate in NiW/Al_2O_3 than that of molybdenum in alumina-supported CoMo or NiMo. The explanation is often reported to be the relatively strong W—O—Al bond [53]. Alternatively, Van Der Vlies et al. [51,52] have pointed out that the W—O bond is stronger than the Mo—O bond, consequently requiring higher temperatures to fully transform tungsten oxide to tungsten sulfide.

The nickel sulfidation rapidly starts at room temperature to form Ni_xS_y phase. The NiWS phase is not observed at low temperatures (20 and 100 °C). For temperatures higher than 200 °C, the proportion of the NiWS phase is predominant and continues slightly to evolve until 400 °C. The quantity of NiWS phase in the case of heteropolyanion based catalyst is larger than in the case of conventional precursor for temperatures varying between 200 and 400 °C. This is due to the proximity of Ni and W in the heteropolyanion as mentioned in a previous study [7]. The quantity of oxysulfide phase is also more important for the catalyst based on heteropolyanion. In agreement with Hensen et al. [27], this phase is found to be a precursor to the active phase NiWS. The results obtained by EPR spectroscopy, correlated with data obtained by XPS and Raman spectroscopy, are consistent with the existence of a Ni^{2+}specie in interaction with the oxysulfide phase. This phase could be sulfided to NiWS phase for temperatures greater than 200 °C.

Whatever the solid, we observed that the sulfidation of tungsten and nickel atoms did not occur at the same temperature. Indeed, the tungsten sulfidation slightly began from 200 °C while the nickel sulfidation starts at room temperature. The use of heteropolyanion

precursor did not alter the sulfidation temperature of both elements (Ni and W). However, a better sulfidation of tungsten and nickel atoms respectively to WS_2 and NiWS phases occurred for HPA precursor, which can be related to the proximity of Ni and W in the heteropolyanion salt maintained after drying.

5. Conclusions

The genesis of ASA-supported NiW catalysts was studied by a combination of XPS spectroscopy, HRTEM, Raman and EPR spectroscopies in order to obtain more information about the nature of the present species as well as the evolution of their proportions versus temperature. Concerning the sulfidation of tungsten atom, we have shown that the oxidic phase is sulfided in WS_2 phase via oxysulfide WO_xS_y and WS_3 intermediates. Whatever the catalyst, the tungsten begins to sulfide in low proportion at 200 °C but the sulfidation is more efficient from 300 °C. The WS_3 phase appears later for the conventional catalyst (300 °C) compared to the heteropolyanion precursor (200 °C). For both catalysts, this latter phase is still present at 400 °C. The nickel atoms are sulfided at room temperature as Ni_xS_y phase but the NiWS phase appears from 200 °C. Whatever the temperature, the proportion of the NiWS phase is predominant on the HPA based catalyst. This can be explained by the more important quantity of oxysulfide phase present in the HPA based catalyst. This phase is proposed to be in interaction with Ni species as suggested by EPR analysis and could be considered as a precursor of the NiWS active phase. However, for both catalysts, the sulfidation of nickel and tungsten elements does not occur at the same temperature. Indeed, the sulfidation of Ni is finished whereas all the W atoms are not yet transformed into WS_2. At 400 °C the sulfidation of Ni and W in the NiSiW11 catalyst is better than on the reference catalyst with 77% of tungsten as WS_2 and 42% of nickel as NiWS. For the conventional catalyst, the optimal temperature of sulfidation is reached at 300 with 49% of WS_2 and 37% of NiWS. Whatever the sulfidation temperature, the NiSiW11 catalyst shows a better sulfidation of both elements (Ni and W) compared to the conventional catalyst. This can be related to the proximity of nickel and tungsten elements in the heteropolyanion salt hence highlighting the importance of using HPA precursor.

Acknowledgements

We are thankful to Nadia Touati and Martine Trentesaux for their respectively help in spectroscopy EPR and XPS. The HRTEM facility in Lille (France) is supported by the Conseil Regional du Nord-Pas de Calais, and the European Regional Development Fund (ERDF).

References

[1] C. Marcilly, Catalyse acido-basique-Application au raffinage et à la pétrochimie, Edition Technip 2 (2003) 693–739.
[2] N.Y. Topsoe, H. Topsoe, Journal of Catalysis 75 (1982) 354–374.
[3] A.M. Maitra, N.W. Cant, Applied Catalysis 48 (1989) 187–197.
[4] J.A.R. Van Veen, P.A.J.M. Hendriks, R.R. Andrea, E.J.G.M. Romers, A.E. Wilson, Journal of Physical Chemistry 94 (1990) 5282–5285.
[5] K. Ben Tayeb, C. Lamonier, M. Fournier, E. Payen, F. Bertoncini, A. Bonduelle, American Chemical Society Division Fuel Chemistry 53 (2008) 9–12.
[6] K. Ben Tayeb, C. Lamonier, C. Lancelot, M. Fournier, E. Payen, F. Bertoncini, A. Bonduelle, Comptes Rendus Chimie 12 (2009) 692–698.
[7] K. Ben Tayeb, C. Lamonier, C. Lancelot, M. Fournier, E. Payen, F. Bertoncini, A. Bonduelle, Catalysis Today 150 (2010) 207–212.
[8] C. Martin, C. Lamonier, M. Fournier, O. Mentré, V. Harlé, D. Guillaume, E. Payen, Chemistry of Materials 17 (2005) 4438–4448.
[9] C. Lamonier, C. Martin, J. Mazurelle, V. Harlé, D. Guillaume, E. Payen, Applied Catalysis B 70 (2007) 548–556.
[10] J. Mazurelle, C. Lamonier, C. Lancelot, E. Payen, C. Pichon, D. Guillaume, Catalysis Today 130 (2008) 41–49.
[11] B. Guichard, M. Roy-Auberger, E. Devers, C. Pichon, C. Legens, P. Lecour, Catalysis Today 149 (2010) 2–10.
[12] B. Guichard, M. Roy-Auberger, E. Devers, C. Legens, P. Raybaud, Catalysis Today 130 (2008) 97–108.
[13] A. Gandubert, C. Legens, D. Guillaume, S. Rebours, E. Payen, Oil & Gas Science and Technology 62 (2007) 79–89.
[14] M. Sun, T. Burgi, R. Cattaneo, D. Van Langeveld, R. Prins, Journal of Catalysis 201 (2001) 258–269.
[15] H.R. Reinhoudt, E. Crezee, A.D. Van Langeveld, P.J. Kooyman, J.A.R. Van Veen, J.A. Moulijn, Journal of Catalysis 196 (2000) 315–329.
[16] D. Eliche-Quesada, J. Mérida-Robles, P. Maireles-Torres, E. Rodriguez-Castellon, G. Busca, E. Finocchio, A. Jiménez-Lopez, Journal of Catalysis 220 (2003) 457–467.
[17] C.H. Kim, W.L. Yoon, I.C. Lee, S.I. Woo, Applied Catalysis A 144 (1996) 159–175.
[18] D. Zuo, D. Li, H. Nie, Y. Shi, M. Lacroix, M. Vrinat, Journal of Molecular Catalysis A 211 (2004) 179–189.
[19] R. Palcheva, A. Spojakina, G. Tyuliev, K. Jiratova, L. Petrov, Kinetics and Catalysis 48 (2007) 847–852.
[20] A. Benitez, J. Ramirez, J.L.G. Fierro, A. Lopez Agudo, Applied Catalysis A 144 (1996) 343–364.
[21] M. Breysse, M. Cattenot, T. Decamp, R. Frety, C. Gachet, M. Lacroix, C. Leclercq, L. De Mourgues, J.L. Portefaix, M. Vrinat, M. Houari, J. Grimblot, S. Kasztelan, J.P. Bonnelle, S. Housni, J. Bachelier, J.C. Duchet, Catalysis Today 4 (1988) 39–55.
[22] L. Coulier, G. Kishan, J.A.R. Van Veen, J.W. Niemantsverdriet, Journal of Physical Chemistry B 106 (2002) 5897–5906.
[23] B. Pawelec, R. Mariscal, J.L.G. Fierro, A. Greenwood, P.T. Vasudevan, Applied Catalysis A 206 (2001) 295–307.
[24] Y. Van Der Meer, E.J.M. Hensen, J.A.R. Van Veen, A.M. Van Der Kraan, Journal of Catalysis 228 (2004) 433–446.
[25] S.D. Kelly, N. Yang, G.E. Mickelson, N. Greenlay, E. Karapetrova, W. Sinkler, S.R. Bare, Journal of Catalysis 263 (2009) 16–33.
[26] M. Sun, D. Nicosia, R. Prins, Catalysis Today 86 (2003) 173–189.
[27] E.J.M. Hensen, Y. Van Der Meer, J.A.R. Van Veen, J.W. Niemantsverdriet, Applied Catalysis A 322 (2007) 16–32.
[28] W. Eltzner, M. Breysse, M. Lacroix, M. Vrinat, Polyhedron 5 (1986) 203–210.
[29] D. Eliche-Quesada, J. Mérida-Robles, P. Maireles-Torres, E. Rodriguez-Castellon, A. Jiménez-Lopez, Applied Catalysis A 262 (2004) 111–120.
[30] N. Frizi, P. Blanchard, E. Payen, P. Baranek, C. Lancelot, M. Rebeilleau, C. Dupuy, J.P. Dath, Catalysis Today 130 (2008) 32–40.
[31] N. Frizi, P. Blanchard, E. Payen, P. Baranek, M. Rebeilleau, C. Dupuy, J.P. Dath, Catalysis Today 130 (2008) 272–282.
[32] D. Ouafi, F. Mauge, J.C. Lavalley, E. Payen, S. Kasztelan, M. Houari, J. Grimblot, J.P. Bonnelle, Catalysis Today 4 (1988) 23–37.
[33] M.J. Vissenberg, Y. Van Der Meer, E.J.M. Hensen, V.H.J. De Beer, A.M. Van Der Kraan, R.A. Van Santen, J.A.R. Van Veen, Journal of Catalysis 198 (2001) 151–163.
[34] S. Kaztelan, Langmuir 6–3 (1990) 590–595.
[35] M. Daage, R.R. Chinelli, Journal of Catalysis 149 (1994) 414–427.
[36] E. Payen, S. Kasztelan, J. Grimblot, J.P. Bonnelle, Catalysis Today 4 (1988) 57–70.
[37] E. Diemman, A. Muller, Coordination Chemistry Reviews 10 (1973) 79–122.
[38] H.R. Reinhoudt, Y. Van der Meer, A.M. Van der Kraan, A.D. Van Langeveld, J.A. Moulijn, Fuel Processing Technology 61 (1999) 43–54.
[39] O.F. Schirmer, E. Salje, Solid State Communications 33 (1980) 333–336.
[40] W. Grunert, W. Morke, R. Feldhaus, K. Anders, Journal of Catalysis 117 (1989) 485–494.
[41] A. Punnoose, M.S. Seehra, Catalysis Letters 78 (2002) 157–160.
[42] C. Sanchez, J. Livage, J.P. Launay, M. Fournier, Journal of the American Chemical Society 105 (1983) 6817–6823.
[43] G.E. Pake, Paramagnetic Resonance, W.A. Benjamin, New York, 1962.
[44] L. Bonneviot, D. Olivier, M. Che, Journal of the Chemical Society, Chemical Communications (1982) 952–953.
[45] M. Kermarec, D. Olivier, M. Richard, M. Che, F. Bozon-Verduraz, Journal of Physical Chemistry 86 (1982) 2818–2827.
[46] A.M. Prakash, L. Kevan, Journal of Physical Chemistry 100 (1996) 19587–19594.
[47] Z. Chang, Z. Zhu, L. Kevan, Journal of Physical Chemistry B 103 (1999) 9442–9449.
[48] G. Kishan, L. Coulier, V.H.J. De Beer, J.A.R. Van Veen, J.W. Niemantsverdriet, Journal of Catalysis 196 (2000) 180–189.
[49] K.T. Ng, D.M. Hercules, Journal of Physical Chemistry 80 (1976) 2094–2102.
[50] A. Benitez, J. Ramirez, A. Vazquez, D. Acosta, A. Lopez Agudo, Applied Catalysis A 133 (1995) 103–119.
[51] A.J. Van Der Vlies, G. Kishan, J.W. Niemantsverdriet, R. Prins, Th. Weber, Journal of Physical Chemistry B 106 (2002) 3449–3457.
[52] A.J. Van Der Vlies, R. Prins, Th. Weber, Journal of Physical Chemistry B 106 (2002) 9277–9285.
[53] B. Scheffer, P.J. Mangnus, J.A. Moulijn, Journal of Catalysis 121 (1990) 18–30.